0026-895X/06/6904-1194–1206$20.00
MOLECULAR PHARMACOLOGY
Copyright © 2006 The American Society for Pharmacology and Experimental Therapeutics
Mol Pharmacol 69:1194–1206, 2006

Vol. 69, No. 4
19299/3099070
Printed in U.S.A.

Discovery of Naturally Occurring Splice Variants of the Rat Histamine H_3 Receptor That Act as Dominant-Negative Isoforms

Remko A. Bakker,[1] Adrian Flores Lozada, André van Marle, Fiona C. Shenton, Guillaume Drutel,[2] Kaj Karlstedt, Marcel Hoffmann,[3] Minnamaija Lintunen, Yumiko Yamamoto, Richard M. van Rijn, Paul L. Chazot, Pertti Panula, and Rob Leurs

The Leiden/Amsterdam Center for Drug Research, Department of Medicinal Chemistry, Vrije Universiteit Amsterdam, Amsterdam, The Netherlands (R.A.B., A.v.M., G.D., M.H., R.M.v.R., R.L.); the Department of Biology, Åbo Akademi University, Turku, Finland (A.F.L., K.K., M.L., Y.Y., P.P.); the Neuroscience Center and Institute of Biomedicine/Anatomy, University of Helsinki, Helsinki, Finland (P.P.); and the School of Biological and Biomedical Sciences, University of Durham, Durham, United Kingdom (F.C.S., P.L.C.)

Received September 26, 2005; accepted December 21, 2005

ABSTRACT

We described previously the cDNA cloning of three functional rat histamine H_3 receptor (rH_3R) isoforms as well as the differential brain expression patterns of their corresponding mRNAs and signaling properties of the resulting rH_{3A}, rH_{3B}, and rH_{3C} receptor isoforms (*Mol Pharmacol* **59:**1–8). In the current report, we describe the cDNA cloning, mRNA localization in the rat central nervous system, and pharmacological characterization of three additional rH_3R splice variants (rH_{3D}, rH_{3E}, and rH_{3F}) that differ from the previously published isoforms in that they result from an additional alternative-splicing event. These new H_3R isoforms lack the seventh transmembrane (TM) helix and contain an alternative, putatively extracellular, C terminus (6TM-rH_3 isoforms). After heterologous expression in COS-7 cells, radioligand binding or functional responses upon the application of various H_3R ligands could not be detected for the 6TM-rH_3 isoforms. In contrast to the rH_{3A} receptor ($rH_{3A}R$), detection of the rH_{3D} isoform using hemagglutinin antibodies revealed that the rH_{3D} isoform remains mainly intracellular. The expression of the $rH_{3D\text{-}F}$ splice variants, however, modulates the cell surface expression-levels and subsequent functional responses of the 7TM H_3R isoforms. Coexpression of the $rH_{3A}R$ and the rH_{3D} isoforms resulted in the intracellular retention of the $rH_{3A}R$ and reduced $rH_{3A}R$ functionality. Finally, we show that in rat brain, the H_3R mRNA expression levels are modulated upon treatment with the convulsant pentylenetetrazole, suggesting that the rH_3R isoforms described herein thus represent a novel physiological mechanism for controlling the activity of the histaminergic system.

Histamine receptors are members of the superfamily of seven transmembrane domain (7TM) G-protein-coupled receptors (GPCRs). The histamine H_3 receptor (H_3R) was pharmacologically identified in 1983 and holds great promise as a target for the development of therapeutics for numerous disorders, including obesity, epilepsy, and such cognitive diseases as attention deficit hyperactivity disorder and Alzheimer's disease (see Bakker, 2004; Leurs et al., 2005 for reviews). The cloning of the H_3R cDNA allowed for the subsequent cloning of related sequences, including a variety of H_3R isoforms from different species (for review, see Bakker, 2004; Leurs et al., 2005).

Alternative splicing of pre-mRNA represents a widespread mechanism for increasing the variability of eukaryotic gene expression by generating structurally distinct isoforms from a single gene. Alterations in the expression of GPCR isoforms could be associated with disease (Schmauss et al., 1993). Although α_1-AR adrenoceptors and dopamine receptors are prime examples of alternatively spliced GPCRs (Cogé et al.,

R.L. is the recipient of a PIONIER award of the Technologiestichting Stichting Technische Wetenschappen of the Nederlandse Organisatie voor Wetenschappelijk Onderzoek. Supported by the Academy of Finland (P.P.), and the Finnish Foundation for Alcohol Studies (P.P., M.L., and A.F.L.).

[1] Current affiliation: Department of Metabolic Diseases, Boehringer Ingelheim Pharma GmbH, Biberach, Germany.
[2] Current affiliation: Institut François Magendie, Bordeaux, France.
[3] Current affiliation: Galapagos Genomics BV, Leiden, The Netherlands.

Article, publication date, and citation information can be found at http://molpharm.aspetjournals.org.
doi:10.1124/mol.105.019299.

ABBREVIATIONS: 7TM, seven transmembrane domain; GPCR, G-protein-coupled receptor; H_3R, histamine H_3 receptor; PTZ, pentylenetetrazole; HA, hemagglutinin; HEK, human embryonic kidney; GTPγS, guanosine 5′-*O*-(3-thio)triphosphate; APT, aminopotentidine; ^{125}IPP, [^{125}I]iodophenpropit; ELISA, enzyme-linked immunosorbent assay; FRET, fluorescence resonance energy transfer; BS3, bis(sulfosuccinimidyl)suberate; PCR, polymerase chain reaction; CREB, cAMP-responsive element-binding protein; *tr*-FRET, time-resolved fluorescence resonance energy transfer; ER, endoplasmic reticulum; 7TM-rH_3R isoforms, the rH_{3A}, rH_{3B}, and rH_{3C} receptors; 6TM-rH_3R isoforms, the rH_{3D}, rH_{3E}, and rH_{3F} isoforms.

1999; Kilpatrick et al., 1999; Hawrylyshyn et al., 2004), more and more GPCR splice variants are identified for other members of the GPCR superfamily. A variety of H_3R isoforms from several species has been reported (for review, see Bakker, 2004; Leurs et al., 2005). In addition to the 445 amino acids containing $rH_{3A}R$, two presumably nonfunctional truncated isoforms (reported as rH_{3T} or $rH_{3(nf1)}$ and $rH_{3(nf2)}$) (Drutel et al., 2001; Morisset et al., 2001) and three functional rH_3R isoforms have been detected: rH_{3B}, rH_{3C}, and the $rH_{3(410)}$ receptor, generated by deletions in the third intracellular loop of the rH_3R of 32, 48, and 35 amino acids, respectively. Because several H_3R isoforms have been shown to possess specific pharmacological characteristics in terms of ligand-binding and initiation of signal-transductions events (Drutel et al., 2001), the H_3R mRNA splicing can significantly affect cellular responses to histamine. A detailed understanding of the spectrum of H_3R splice variants in different species is of importance not only for the understanding of histaminergic system, but also for future drug development efforts.

In the present study, we describe the identification of three additional 6TM-rH_3 isoforms after an RT-PCR approach using rat brain cDNA. Although the mRNA for these 6TM-rH_3 isoforms is detected in the rat brain, in attempting their characterization, we failed to detect radioligand binding using H_3R specific radioligands as well as functional effects upon heterologous expression in COS-7 cells. Coexpression of 7TM-rH_3Rs with the 6TM-rH_3 isoforms, however, revealed that the 6TM-rH_3 isoforms inhibit the cell surface trafficking and subsequent functional activity of the 7TM-rH_3Rs. The regulation of the expression of the 6TM-rH_3 isoforms may therefore represent a novel mechanism for the regulation of H_3R functionality. To study possible in vivo functional relationships between 7TM-rH_3R and 6TM-rH_3 isoforms, relative expression levels were analyzed in a model of generalized tonic-clonic seizures induced by pentylenetetrazole (PTZ). Data from a study on kainic acid-induced status epilepticus indicates that systemic kainic acid induces a direct or indirect selective increase in H_3R isoforms with a full third intracellular loop in areas that suffer rapid neuronal damage (Lintunen et al., 2005). No data are currently available regarding whether 7TM-rH_3R and 6TM-rH_3 isoforms are similarly regulated under pathophysiological conditions in the rat brain. The PTZ seizure model used in this study allows us to determine whether an H_3R isoform-specific response occurs in a pathological setting. Our findings therefore uncover a new mechanism that may control the regulation of H_3R activity in the brain.

Materials and Methods

Materials. Immepip, clobenpropit, and thioperamide were synthesized at the department of Medicinal Chemistry at the Vrije Univeristeit Amsterdam. Gifts of $pcDEF_3$ (Dr. J. Langer, Robert Wood Johnson Medical School, Piscataway, NJ), pTLN21CRE-Luc (Dr. W. Born, National Jewish Medical and Research Center, Denver, CO), and of the cDNAs encoding the PTX-insensitive mutant rat $G\alpha_{i/o}$ proteins $G\alpha_{i1}C^{351}I$, $G\alpha_{i2}C^{352}I$, $G\alpha_{i3}C^{351}I$, and $G\alpha_oC^{351}I$ (Dr. G. Milligan, University of Glasgow, Glasgow, UK), the cDNA encoding the FLAG-tagged $rH_{3A}R$ (Dr. F. Cogé, Institut de Recherches Servier, Croissy sur Seine, France), the cDNA encoding the human histamine H_1 receptor (Dr. H. Fukui, University of Tokushima, Tokushima, Japan), the cDNA encoding the KSHV-GPCR ORF74 (Dr. T. Schwartz, University of Copenhagen, Copenhagen, Denmark), mianserin hydrochloride (Organon NV, The Netherlands), and the HA antibody and rhodamine-labeled secondary antibody (Dr. J. van Minnen, Vrije Universiteit, Amsterdam, The Netherlands), are greatly acknowledged. All other materials were from commercial suppliers.

Constructs. The reverse transcription and PCR amplification for cloning of the $rH_{3D\text{-}F}$ (6TM-rH_3) isoform cDNAs were performed as described previously (Drutel et al., 2001). The full-length cDNAs were isolated with primers overlapping the rat H_3R cDNA sequence. The forward sequence included a Kozak sequence (underlined) (5′-CCG CCA CCA TGG AGC GCG CGC CGC CCG ACG GGC TG-3′). The reverse sequence was based on cDNA for rat orphan GPCR (Genbank accession number AB015646) (5′-CTC TAC CCC ATA ACC ACC CAC C-3′). The use of these primers resulted in the amplification of at least three different products. After cloning in pCRII-TOPO, the cDNAs were sequenced on both DNA strands and subcloned in $pcDNA_3$. The sequence of the identified rH_{3F} isoform is identical to one of the sequences found in the GenBank database (accession number AB015646; GI: 6681587), the sequences of the rH_{3D} and rH_{3E} isoforms have been deposited in the GenBank database (accession numbers DQ112342 and DQ112343, respectively). The hydropathic profile of the $H_{3D\text{-}F}$ isoforms was analyzed using the TMHMM Server at the Center for Biological Sequence Analysis, Technical University of Denmark, DTU, Lyngby, Denmark (http://www.cbs.dtu.dk/services/TMHMM/).

Construction of rH_3R-Gα Protein Fusion Constructs. Fusion proteins between the rat H_3R and PTX-insensitive mutant rat Gα-proteins of the $G_{i/o}$ class were created by PCR using Turbo Pfu to remove the translation initiation codon from the Gα-protein cDNA sequence and the stop codon from the $rH_{3A}R$ cDNA sequence.

HA-Tagging of the rH_3R Isoforms. N-Terminal hemagglutinin (HA)-tagged expression constructs of the $rH_{3A}R$ and rH_{3D} isoform were generated by PCR (5′-GCC ACC ATG GGC TAC CCA TAC GAC GTC CCA GAC TAC GCC GCG GAG CGC GCG CCG C-3′) and cloned into pcDNA 3.1 (Invitrogen, Leek, The Netherlands). Construct integrity was verified by sequence analysis.

Animals. The study was conducted in accordance with the European Convention (1986) guidelines and approved by the local committee for Animal Experiments and the Provincial State Office of Western Finland and the Animal Ethics Committee of Abo Akademi University. Male Sprague-Dawley rats (260–280 g) were given PTZ (50 mg/kg, i.p.). Animals were stunned with CO_2 and killed by decapitation 6 h (PTZ, $n = 3$), 24 h (PTZ, $n = 3$), and 48 h (PTZ, $n = 3$; saline control, $n = 3$) after injection.

In Situ Hybridization Histochemistry. Probes were labeled with deoxy-[α-^{33}P]ATP (PerkinElmer Life and Analytical Sciences, Boston, MA) at their 3′ ends using terminal deoxynucleotide transferase (Promega, Madison, WI), and subsequent in situ hybridization histochemistry was performed essentially as described previously (Drutel et al., 2001). The following oligo-probe sequence was used for detecting H_{3DEF} isoform mRNAs: 5′-AAG TTT CCC GAG GCG CTC GAC ACA GTA ATC GGG GAT GCA GCG GCC-3′.

Image Analysis and Data Interpretation. Autoradiographic films were quantified by digitizing the film images using the MCID 5+ image analysis system (Imaging Research, St. Catherines, ON, Canada) and by measuring gray scale pixel values. The relative optic density was converted to integrated optic density based on a curve derived from ^{14}C standards exposed to films. Gray scale values were determined by using a total of four sections for each animal.

Cell Culture and Transfection. African green monkey kidney COS-7 cells were maintained and transfected as described previously (Drutel et al., 2001; Bakker et al., 2004a). HEK 293 cells were cultures under similar conditions and transfected with cDNA encoding the $rH_{3A}R$ using the LipofectaminePlus method according to the manufacturer's protocols.

Reporter-Gene Assay. H_3R isoform-mediated modulation of cAMP mediated gene transcription activity was measured using the

luciferase reporter-gene plasmid pTLNC121–3 (2.5 μg/10^6 cells) containing 21 cAMP-responsive elements. Luminescence was assayed 48 h after incubation of transfected cells with ligands as described previously (Bakker et al., 2004b).

[^{35}S]GTPγS Binding Assays. Transfected COS-7 cells were resuspended in 4°C binding buffer (20 mM HEPES, 3 μM GDP, 10 mM $MgCl_2$, and 150 mM NaOH, pH 7.4). For measurement of agonist-stimulated GTPγS binding, 6 μg of the crude cell extract was incubated in binding buffer with ligands for 15 min at 30°C after which 0.1 to 0.2 nM [^{35}S]GTPγS (1250 Ci/mmol; PerkinElmer Life and Analytical Sciences) was added to make a final total volume of 100 μl. Bound radioactivity was separated by filtration after 15 min through Whatman GF/C filters on a Brandel cell harvester using 4°C wash buffer (20 mM HEPES and 5 mM $MgCl_2$, pH 7.4). Radioactivity retained on the filters was measured by liquid scintillation counting.

Receptor Binding Studies. Radioligand binding studies for the H_1R, H_2R, and H_3R using [^{3}H]mepyramine, [^{125}I]aminopotentidine, and [N^α-methyl-^{3}H]histamine, respectively, were performed as described previously (Bakker et al., 2004b). The H_3R radioligand binding studies using [^{125}I]iodophenpropit (^{125}IPP) were carried out under the same experimental conditions as for [N^α-methyl-^{3}H]histamine. CXCL8 was labeled with ^{125}I using the Iodogen method (Pierce, Rockford, IL) and subsequently used in ORF74 radioligand binding studies as described previously (Smit et al., 2002).

Detection of Tagged rH$_3$Rs. In the enzyme-linked immunosorbent assays (ELISA), a mouse anti-HA monoclonal primary antibody was used as primary antibody, and a goat anti-mouse–horseradish peroxidase conjugate as secondary antibody for the detection of tagged rH$_3$Rs in transfected cells. The 3,3′-, 5,5′-tetramethylbenzidine liquid substrate system for ELISA was used as substrate and the optical density was measured at 450 nm using a Victor^2 Wallac multilabel counter (PerkinElmer Life and Analytical Sciences). The same primary antibody was used for immunocytochemistry in conjunction with a secondary rhodamine labeled goat-anti-mouse antibody. Permeabilization of cells was achieved by an optional incubation of the cells for 5 min with 0.5% Nonidet P-40 in TBS before antibody application. For imaging, coverslips were mounted in 90% glycerol containing 0.02 M Tris-HCl, pH 8.0, 0.002% NaN_3, and 2% 1,4-diazabicyclo-(2,2,2)-octane (Merck, Darmstadt, Germany).

Time-Resolved FRET. The time-resolved fluorescence resonance energy transfer (FRET) experiments were conducted essentially as described previously (Bakker et al., 2004a). Energy transfer was measured by exciting the Eu^{3+} at 320 nm and monitoring the allophycocyanin emission for 1 ms at 665 nm using a Novostar (BMG LABTECH GmbH, Offenburg, Germany) configured for time-resolved fluorescence after a 50-μs delay.

Cross-Linking and Immunoblotting of rH$_{3A}$ Receptors. Cells were harvested by centrifugation, and the resulting pellet was resuspended in 150 μl of cross-linking buffer (150 mM NaCl, 100 mM Na-HEPES, 5 mM EDTA, pH 7.5, and 5 mM DTT) to give a final protein concentration of approximately 0.5 mg/ml. The samples were incubated at room temperature with continual mixing for 12 min with either a 0.12 mM or a 0.25 mM concentration of the cell permeable cross-linker bis(sulfosuccinimidyl)suberate (BS3), after which the cross-linking mixture was removed by centrifugation and the resultant pellet was used for immunoblotting as described previously (Chazot et al., 2001). Immunoblots were probed either with anti-H_{3C} 188–197Cys antibody (Shenton et al., 2005) at a 0.2 μg/ml, or with an anti-H_3 329–358 antibody used at a final protein concentration of 1.5 μg/ml (Chazot et al., 2001).

Analytical Methods. All data shown are expressed as mean ± S.E.M. Data from radioligand binding assays and functional assays data were evaluated by a nonlinear, least-squares curve-fitting procedure using Prism (GraphPad Software, Inc., San Diego, CA).

Results

Cloning of cDNAs Encoding Additional Rat H$_3$R Isoforms

The existence of additional H_3R isoforms was investigated by RT-PCR analysis of rat whole-brain total RNA using specific primers 1 and 2 (see *Materials and Methods*), and revealed the existence of three previously uncharacterized full-length cDNAs with putative corresponding proteins of 497 (rH_{3D}), 465 (rH_{3E}), and 449 (rH_{3F}) amino acids. The amino acid sequence of the rH_{3F} isoform corresponds to one of the sequences found in the GenBank database (accession number AB015646; GI: 6681587). These three new rH_3 isoforms correspond in a large part to the sequences of rat histamine H_3R isoforms A, B, and C (rH_{3A}R, rH_{3B}R, and rH_{3C}R, respectively) and exhibit exactly the same differences in length for the third intracellular loop (Fig. 1A). This insertion in the third intracellular loop in the rH_{3D}, rH_{3E}, and rH_{3F} isoforms seems to be created by a retention/deletion system already described for the third intracellular loop (Cogé et al., 2001; Drutel et al., 2001; Morisset et al., 2001). However, the rH_{3D}, rH_{3E}, and rH_{3F} isoforms differ from the rH_{3A}R, rH_{3B}R, and rH_{3C}R in their C-terminal region, in which the last C-terminal 53 amino acids, which correspond to the seventh transmembrane-domain and carboxyl terminus of the rH_{3A}R, rH_{3B}R, and rH_{3C}R proteins, are replaced by a sequence of 105 amino acids that do not share any homology with the last 53 C-terminal amino acids of the rH_{3A}R, rH_{3B}R, and rH_{3C}R. Sequence analysis of the rH_3R gene indicates that the alternative C-terminal domain that is found in the $rH_{3D\text{-}F}$ isoforms is due to a change in the open reading frame upon alternative splicing using previously unidentified exon/intron junctions present within the rH_3R gene (see Fig. 1B). Analysis of the hydropathic profile of the rH_{3D}, rH_{3E}, and rH_{3F} isoforms does not reveal a clear putative seven transmembrane domain (Fig. 2, A and B). Therefore, the rH_{3D}, rH_{3E}, and rH_{3F} isoforms are predicted to possess only six transmembrane domains 6TM-rH_3 isoforms) and an extracellular C-teriminal domain (Fig. 2, C and D).

Heterologous Expression of Epitope-Tagged rH$_3$R Isoforms. We have successfully characterized the rH_{3A}R, rH_{3B}R, and rH_{3C}R using COS-7 cells heterologously expressing these receptors (Drutel et al., 2001). We therefore used the same approach in this study to characterize the three additional 6TM-rH_3 isoforms described herein. To evaluate the cell surface expression of the 6TM-rH_3 isoforms, we generated the cDNAs coding for the N-terminally HA-tagged rH_{3A}R (HA-rH_{3A}R) and the N-terminally HA-tagged rH_{3D} (HA-rH_{3D}) isoform by PCR. Although we detected clear immunological evidence for the cell surface expression of the HA-rH_{3A}R with the use of an ELISA assay using anti HA-antibodies on intact cells, we can hardly detect the HA-rH_{3D} isoforms on the cell surface on intact cells (Fig. 2E). We observe, however, a clear immunofluorescent signal upon permeabilization of cells expressing the HA-rH_{3D} isoform (Fig. 2E), indicating successful synthesis of the HA-tagged rH_{3D} isoform protein and retention of the HA-tagged rH_{3D} isoform inside the cell. There is an apparent difference in detection of the HA-rH_{3D} isoform versus the HA-rH_{3A}R, which might indicate differences in, for example, the rate of synthesis, the inherent stability, or the rate of degradation of the H_3 isoforms, but we have not pursued this issue further. To evaluate the plasma membrane localization of the HA-rH_{3A}R and the HA-rH_{3D} isoform, we subsequently performed immunocy-

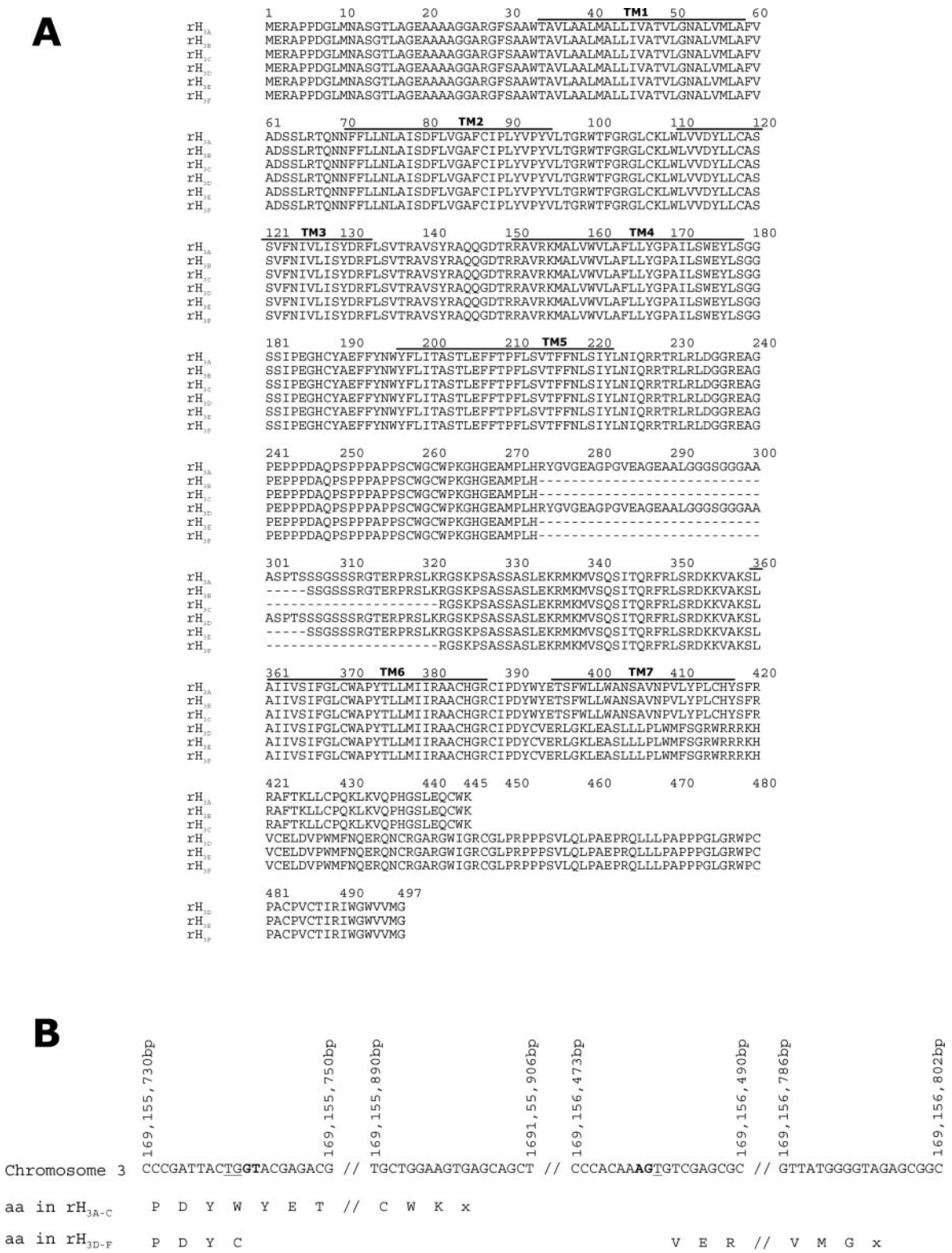

Fig. 1. Sequence alignment of rH_3R isoforms and genomic organization of the rH_3R gene. A, amino acid sequence alignment of various rH_3R isoforms. The $rH_{3B}R$ and $rH_{3C}R$ isoforms exhibit amino acid deletions in the third intracellular loop of the rH_3R protein compared with the full-length $rH_{3A}R$. The rH_{3D}, rH_{3E}, and rH_{3F} isoforms differ from the $rH_{3A}R$, $rH_{3B}R$, and $rH_{3C}R$ isoforms, respectively, in an alternative C-terminal domain as a result of an additional splicing event. Indicated above the amino acids are the seven transmembrane domains as they are found for the $rH_{3A}R$, $rH_{3B}R$, and $rH_{3C}R$ isoforms (TM1 through TM7). B, diagram of the exon/intron structure of the rat H_3R gene on chromosome 3 (Genbank accession number NM_053506.1; GI:16758263) and the resulting amino acid (aa) sequences found in rH_{3A-C} receptors and rH_{3D-E} isoforms generated by retention/deletion of the pseudointrons. The exon/intron junctions within the rH_3R gene are indicated in bold (**GT** and **AG**), whereas the codon that corresponds to the cysteine (C) found in the rH_{3D-F} isoforms (formed by TG and T) is underlined. For simplicity, only part of the exon/intron structure of the rat H_{3R} gene and of the rH_3R gene sequence is shown (indicated by //). See Morisset et al. (2001) for an overview of the exon/intron structure of the rH_3R gene corresponding to the two presumably nonfunctional H_3R isoforms, $H_{3(nf1)}$ and $H_{3(nf2)}$, and the four previously described functional shorter isoforms, rH_{3B} ($rH_{3(413)}$), $rH_{3(410)}$, and rH_{3C} ($rH_{3(397)}$).

tochemistry studies using rhodamine labeled anti-HA antibodies. Plasma membrane localization of the rhodamine-derived fluorescence was easily detected using cells expressing HA-rH_{3A}Rs in intact cells (Fig. 2F, top left) and only a limited intracellular fluorescence was observed in Nonidet P40-permeabilized cells (Fig. 2F, top right). In contrast, corroborating the findings obtained by the ELISA studies, using cells transfected with cDNA encoding the HA-rH_{3D} isoform, appreciable rhodamine-derived fluorescence is detected only in permeabilized cells (Fig. 2F, bottom right) and not on intact cells (Fig. 2F, bottom left). Moreover, no plasma membrane localization of the rhodamine-derived fluorescence was detected using permeabilized HA-rH_{3D} isoform-expressing cells. These data indicate an intracellular localization for the HA-rH_{3D} isoform.

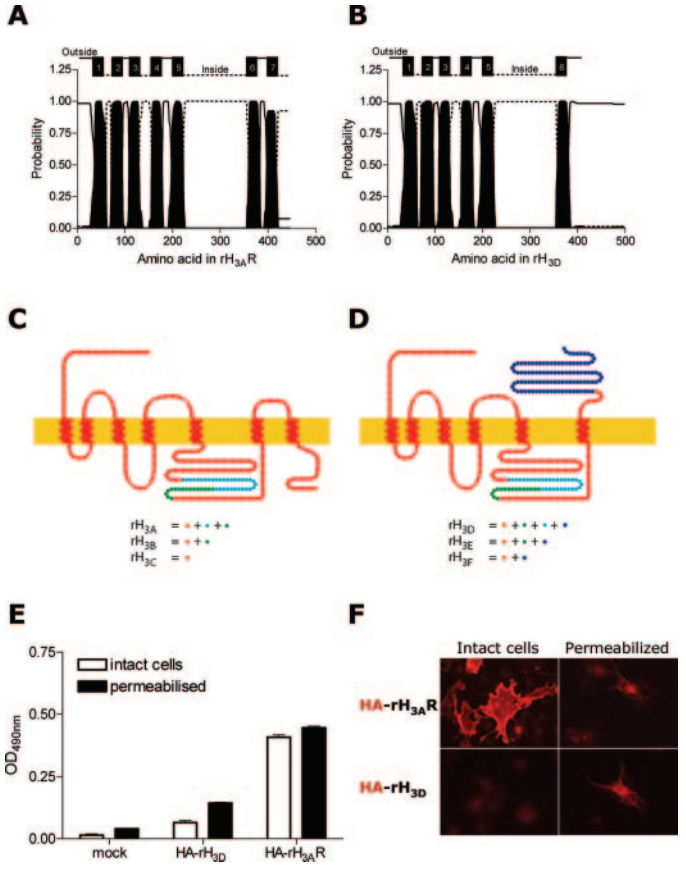

Fig. 2. Topology of the rH_3R isoforms. Prediction of the topology of the $rH_{3A}R$ (A) versus the $rH_{3D}R$ (B), as predicted by the TMHMM Server at the Center for Biological Sequence Analysis, Technical University of Denmark, DTU (http://www.cbs.dtu.dk/services/TMHMM/). Indicated by the solid line are the probabilities for localization on the extracellular side (outside); the probabilities of localization on the intracellular side (inside) are indicated by the dotted lines. The probability for transmembrane (TM) domains are indicated by the filled areas. From these two plots, it can be deduced that seven TM domains are predicted for the $rH_{3A}R$, whereas for the $rH_{3D}R$, only six TM domains are predicted, as indicated above the graphs. C, graphical representation of the topology of the rH_{3A}, rH_{3B}, and rH_{3C} receptors, versus the rH_{3D}, rH_{3E}, and rH_{3F} isoforms (D). In contrast to the rH_{3A}, rH_{3B}, and rH_{3C} receptors, the rH_{3D}, rH_{3E}, and rH_{3F} isoforms are predicted to possess an extracellular C-terminal domain. Also indicated in C and D are the variations in the third intracellular loop between the isoforms. E and F, immunological detection of N-terminally HA-tagged rH_{3A}Rs (HA-rH_{3A}) and the N-terminally HA-tagged rH_{3D} isoform (HA-rH_{3D}) on transfected COS-7 cells. E, Detection of HA-rH_{3A}Rs and the HA-rH_{3D} isoform in intact cells versus cells that have been permeabilized using 0.5% Nonidet P-40 in an ELISA assay. F, immunocytochemical detection of HA-tagged rH_3R isoforms using a rhodamine conjugated antibody directed against the HA-tag. Detection of HA-rH_{3A}Rs on intact COS-7 cells (top left) and in permeabilized cells (top right). Detection of the HA-rH_{3D} isoform on intact cells (bottom left) and in permeabilized cells (bottom right).

Are the 6TM-rH_3 Isoforms Functional H_3Rs?

Radioligand Binding Studies. To evaluate whether the identified mRNA species for the 6TM-rH_3 isoforms code for functional H_3Rs, we transfected COS-7 cells with the cDNA encoding either the $rH_{3A}R$ or one of the 6TM-rH_3 isoforms and evaluated corresponding membrane preparations for their ability to bind either the inverse H_3R agonist radioligand ^{125}IPP or the H_3R agonist radioligand [N^{α}-methyl-^{3}H]histamine. Cell homogenates derived from cells expressing the $rH_{3A}R$ bind ^{125}IPP with high affinity (K_D = 2.1 nM, B_{max} = 2.5 pmol/mg of protein) and exhibits the expected affinities for IPP, immepip, and thioperamide (pK_b for ^{125}IPP, 8.2 ± 0.1; pK_i values for immepip and thioperamide, 6.5 ± 0.2 and 7.7 ± 0.1, respectively). In contrast, we failed to detect specific ^{125}IPP-binding to cells transfected with cDNAs coding for any of the 6TM-rH_3 isoforms (Fig. 3A). Likewise, we did not detect [N^{α}-methyl-^{3}H]histamine binding to membranes of cells transfected with cDNAs encoding the 6TM-rH_3 isoforms (data not shown).

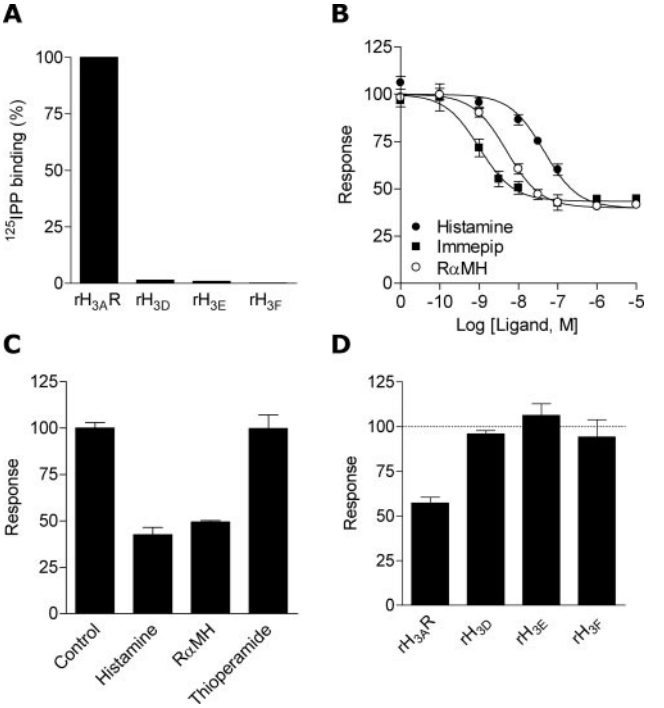

Fig. 3. Functional analysis of the $rH_{3A}R$ and the rH_{3D} isoform upon transient transfection of their corresponding cDNAs in COS-7 cells. A, transfection of cells with $rH_{3A}R$ coding cDNA (pcDEF$_3$$rH_{3A}R$; 5 mg/$10^6$ cells) resulted in the expression of ^{125}IPP binding sites, whereas no specific ^{125}IPP binding was detected to membrane fractions of cells transfected with an equal amount of cDNA coding for either the rH_{3D}, rH_{3E}, or rH_{3F} isoform. B, dose-dependent modulation of 10 mM forskolin induced responses by histamine, immepip, and $R(\alpha)$-methylhistamine using COS-7 cells cotransfected with 5 mg/10^6 cells of both pcDEF$_3$$rH_{3A}R$ and a CREB-responsive firefly-luciferase reporter gene (pTLNC121CRE). C, modulation of forskolin (10 mM) induced responses by 10 mM histamine, $R(\alpha)$-methylhistamine (RaMH), and thioperamide using cells transfected with both pcDEF$_3$$rH_{3A}R$ and pTLNC121CRE. The forskolin-induced responses are set to 100% as indicated by "control". D, effects of 10 mM $R(\alpha)$-methylhistamine on forskolin (10 mM) induced responses using cells cotransfected with either pcDEF$_3$$rH_{3A}R$, pcDEF$_3$$rH_{3D}$, pcDEF$_3$$rH_{3E}$, or pcDEF$_3$$rH_{3F}$, and pTLN121CRE. The forskolin induced responses are set to 100% as indicated by the dashed line.

Functional Assays. The H_3R couples to members of the $G_{i/o}$ family of G-proteins to inhibit adenylyl cyclase activity and subsequently inhibits the formation of intracellular cAMP (Leurs et al., 2005). Cotransfection of COS-7 cells with the $rH_{3A}R$ encoding cDNA together with pTLN121CRE, a cAMP-responsive element-binding protein (CREB)-responsive firefly-luciferase reporter gene, allowed us to monitor H_3R-induced modulation of forskolin-induced reporter-gene expression. In concert with the $G_{i/o}$-coupled nature of the H_3R (see Leurs et al., 2005), treatment of cotransfected cells with varying concentrations of the H_3R agonists immepip, $R(\alpha)$-methylhistamine, and histamine results in the dose-dependent inhibition of 10 mM forskolin-induced firefly-luciferase expression by approximately 60% with EC_{50} values of approximately 2, 7, and 43 nM, respectively (Fig. 3B), in $rH_{3A}R$-expressing cells. Under these assay conditions, we do not observe constitutive activity for the $rH_{3A}R$ because the inverse H_3R agonist thioperamide (Leurs et al., 2005) is without effect on the forskolin-induced luciferase expression (Fig. 3C). Although 1 mM $R(\alpha)$-methylhistamine potently induces signaling via the $rH_{3A}R$, under the same assay conditions, $R(\alpha)$-methylhistamine is without effect on the forskolin-induced firefly-luciferase expression in cells cotransfected with cDNAs encoding the reporter gene and either of the 6TM-rH_3 isoforms (Fig. 3D).

Is There a Role for the 6TM-rH_3 Isoforms?

Detection of Epitope-Tagged rH_3R Isoforms in Coexpression Studies. The immunological and immunocytochemistry data obtained with the N-terminally HA-tagged HA-rH_{3D} isoform indicates poor plasma membrane expression of the rH_{3D} isoform (Fig. 2, E and F). In addition, in cells transfected with cDNA encoding either of the 6TM-rH_3 isoforms we have been unable to detect 1) specific ^{125}IPP or [N^{α}-methyl-^{3}H]histamine binding (Fig. 3A) and 2) modulation of forskolin-induced transcriptional events that are otherwise modulated by $rH_{3A}R$ activation under the same conditions. In recent years, accumulating evidence suggests that some GPCRs [e.g., the $GABA_B$ receptors (White et al., 1998) and odorant receptors (Hague et al., 2004a)] require particular protein-protein interactions to allow proper plasma membrane expression. It seems that the 6TM-rH_3 isoforms are retained intracellularly; we postulated, therefore, that the additional expression of GPCRs might aid the cell surface expression of the 6TM-rH_3 isoforms. Conversely, the 6TM-rH_3 isoforms may possibly retain the coexpressed GPCRs intracellularly by acting as dominant-negative isoforms.

Do the 6TM-rH_3 Isoforms Interfere with Cell Surface Expression of 7TM-rH_3Rs? We cotransfected COS-7 cells with the cDNAs coding for the HA-$rH_{3A}R$ and the rH_{3D} isoform. Similar to the effects of coexpression of alternative splice variants of human α_{1A}-adrenoceptors (Cogé et al., 1999), we found that the coexpression of the rH_{3D} isoform reduced the expression of the HA-$rH_{3A}R$ at the plasma membrane. This phenomenon is observed using either an ELISA assay on intact cells or by applying immunocytochemistry techniques using a rhodamine labeled anti-HA antibody (Fig. 4, A and B, respectively).

Evaluation of Ligand-Binding Sites upon Coexpression of 7TM-H_3R and 6TM-rH_3 Isoforms. To evaluate whether the loss of HA-$rH_{3A}R$-derived immunofluorescence at the cell surface upon coexpression of the rH_{3D} isoform also results in a loss of ligand binding sites for H_3R ligands we performed radioligand binding assays. As shown in Fig. 3A, ^{125}IPP binding sites are detected upon the expression of 7TM-rH_3Rs (Drutel et al., 2001), such as the $rH_{3A}R$, whereas expression of the 6TM-rH_3 isoforms does not result in the formation of ^{125}IPP binding sites.

The transfection of 0.25 mg/10^6 cells of cDNA coding for the $rH_{3A}R$ resulted in the expression of 2.5 pmol/mg of protein ^{125}IPP binding sites. Coexpression of the $rH_{3A}R$ together with the rH_{3D} isoform, however, resulted in an rH_{3D}-isoform gene-dosage–dependent reduction of $rH_{3A}R$-derived ^{125}IPP binding sites (Fig. 5A); the remaining ^{125}IPP binding sites exhibit a pharmacological indistinguishable from that of the $rH_{3A}R$ (pK_b for ^{125}IPP, 8.1 ± 0.1; pK_i values for immepip and thioperamide, 6.9 ± 0.2 and 7.6 ± 0.1, respectively). The coexpression of the rH_{3E} or rH_{3F} isoform together with the $rH_{3A}R$ resulted in a similar reduction of ^{125}IPP binding sites (Fig. 5, B and C, respectively), indicating that the 6TM-rH_3 isoforms interfere with the expression of the $rH_{3A}R$. The maximal inhibition of ^{125}IPP binding sites (as evaluated by a transfection of cells with an $rH_{3A}R$/6TM-rH_3 isoform cDNA ratio of 1:10) is ~50 to 75% (Fig. 5, A–C). To evaluate whether the observed inhibition of ^{125}IPP binding-site expression is specific for the 6TM-rH_3 isoforms, we performed additional experiments in which we cotransfected cells with the same amount of $rH_{3A}R$ cDNA in combination with various amounts of cDNA encoding the human histamine H_1 receptor (hH_1R) (Fig. 5D). Although the transfection of COS-7 cells with the hH_1R cDNA resulted in the formation of binding-sites for the H_1R radioligand [^{3}H]mepyramine with pharmacological characteristics of the hH_1R (data not

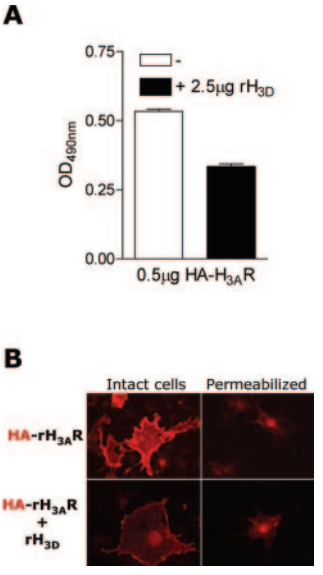

Fig. 4. Immunological detection of N-terminally HA-tagged $rH_{3A}Rs$ (HA-rH_{3A}) on COS-7 cells cotransfected with cDNA coding for HA-rH_{3A} receptors and the N-terminally HA-tagged rH_{3D} isoform (HA-rH_{3D}). A, effects of the cotransfection of pcDEF$_3$-rH_{3D} on the detection of HA-$rH_{3A}Rs$ on intact cells using an ELISA assay. B, immunocytochemical detection of HA-$rH_{3A}Rs$ using a rhodamine conjugated antibody directed against the HA-tag. Detection of HA-$rH_{3A}Rs$ on intact COS-7 cells (top left) and in permeabilized cells (top right), and effects of cotransfection cells with both pcDEF$_3$-HA-rH_{3A} and pcDEF$_3$-rH_{3D} on the detection of the HA-$rH_{3A}Rs$ on intact cells (bottom left) and in permeabilized cells (bottom right). Control slides of cells transfected with N-terminally HA-epitope tagged H_3 isoforms that did not receive the primary antibody or of untransfected cells showed no appreciable staining.

shown), no specific ^{125}IPP binding was detected in hH_1R-expressing cells (Fig. 5D). Cotransfection of cells with cDNAs encoding both the $rH_{3A}R$ and the hH_1R, however, did not influence the formation of ^{125}IPP binding sites.

Similar to the findings with the hH_1R, expression of the rat H_2R (rH_2R) or the viral chemokine receptor from Karposi's sarcoma herpes virus KSHV-GPCR (also known as ORF74) in COS-7 cells resulted in the formation of binding sites for the H_2R radioligand ^{125}IAPT and ^{125}I-CXCL8, a radioligand for ORF74, respectively, but not in the formation of ^{125}IPP binding sites. Coexpression of the $rH_{3A}R$ with either the rH_2R or ORF74, however, did not affect the formation of $rH_{3A}R$-derived ^{125}IPP binding sites (Fig. 5E).

We also evaluated the effects of the coexpression of the $rH_{3B}R$ and $rH_{3C}R$ with the rH_E and rH_F isoforms, respectively, on the formation of ^{125}IPP binding sites. Similar to the expression of the $rH_{3A}R$, expression of the $rH_{3B}R$ or $rH_{3C}R$ in COS-7 cells results in the formation of ^{125}IPP binding sites (Drutel et al., 2001). Coexpression of the $rH_{3B}R$ or $rH_{3C}R$ together with either the rH_{3E} or rH_{3F} isoform resulted in an

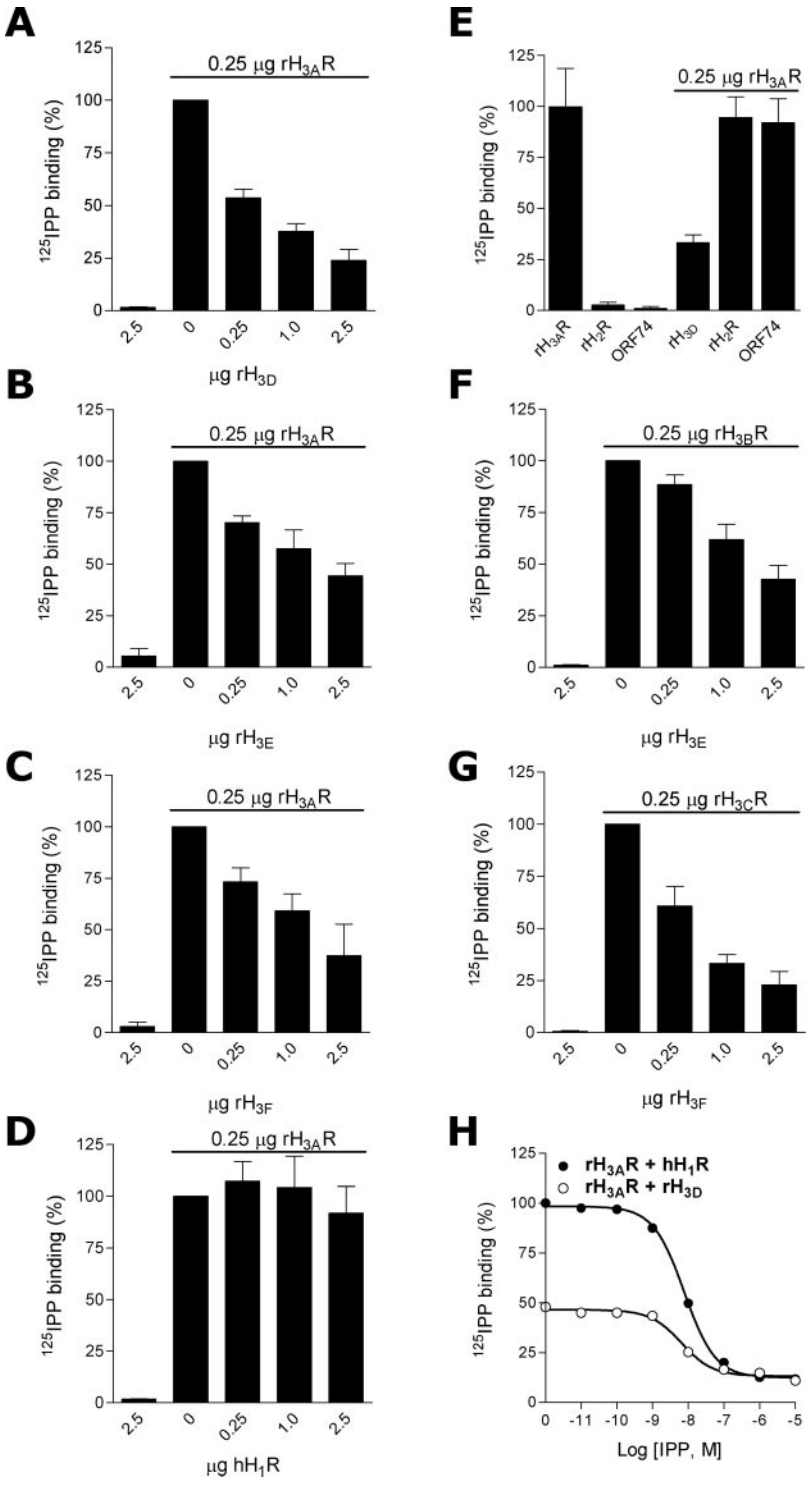

Fig. 5. Effects of cotransfection of cDNA coding for rH_3R isoforms on the expression of ^{125}IPP binding sites. Evaluation of the effects of cotransfection of either 0.25 mg/10^6 cells of $pcDEF_3rH_{3A}R$ (A, B, C, D, and E), $pcDEF_3rH_{3B}R$ (F), or $pcDEF_3rH_{3C}R$ (G) together with varying amounts (0–2.5 mg/10^6 cells) of either $pcDEF_3rH_{3D}$ (A), $pcDEF_3rH_{3E}$ (B and F), $pcDEF_3rH_{3F}$ (C and G), $pcDEF_3hH_1$ (D), $pcDEF_3rH_2R$ (E), or $pcDEF_3$ORF74 (E) on the relative number of expressed ^{125}IPP binding sites. H, evaluation of the effects of cotransfection of $pcDEF_3rH_{3A}R$ (0.25 mg/10^6 cells) together with 2.5 mg/10^6 cells of either $pcDEF_3rH_{3D}$ (○) or $pcDEF_3hH_1$ (●) on the ability of IPP to displace ^{125}IPP bound to expressed ^{125}IPP binding sites (homologous displacement). Also shown in E are the effects of the transfection of 2.5 mg/10^6 cells of either $pcDEF_3rH_{3A}R$, $pcDEF_3rH_2R$, $pcDEF_3$ORF74, or $pcDEF_3rH_{3D}$ alone on the expression of ^{125}IPP binding sites. The proper expression in COS-7 cells of the hH_1R, the rH_2R, and ORF74 was confirmed using [^{3}H]mepyramine, [^{125}I]iodoaminopotentidine, and ^{125}I-CXCL8 binding assays, respectively (data not shown). In each condition, the total amount of cDNA has been kept constant using $pcDEF_3$.

rH_{3E} isoform and rH_{3F} isoform gene-dosage dependent reduction of $rH_{3B}R$-derived (Fig. 5F) and $rH_{3C}R$-derived (Fig. 5G) ^{125}IPP binding sites, respectively. The maximal inhibition of ^{125}IPP binding sites, as evaluated by a transfection of cells with an $rH_{3B}R$ or $rH_{3C}R$-to-6TM-rH_3 isoform cDNA ratio of 1:10 is ~50 to 75% (Fig. 5, F and G), similar to our findings on the coexpression of the $rH_{3A}R$ with the 6TM-rH_3 isoforms (Fig. 5, A–C).

Although the coexpression of the $rH_{3A}R$ with the rH_{3D} isoform inhibits the formation of ^{125}IPP binding sites, the remaining ^{125}IPP binding sites exhibit unchanged pharmacological characteristics of the $rH_{3A}R$, as evidenced by its unchanged affinity for IPP (Fig. 5H). Taken together, these radioligand-binding data clearly demonstrate that the expression of the 6TM-rH_3 isoforms selectively interferes with the expression of the 7TM-rH_3Rs.

Evaluation of H_3R Ligand-Induced [^{35}S]GTPγS Binding upon Coexpression of 7TM-H_3R and 6TM-rH_3 Isoforms

Creation of $rH_{3A}R$ Gα Fusion Proteins. Because we failed to detect H_3R-agonist mediated [^{35}S]GTPγS binding to activated Gα proteins in cell membranes derived from 6TM-rH_3 isoform expressing cells (data not shown), we chose to evaluate H_3R-agonist induced [^{35}S]GTPγS binding to assess the effects of the coexpression of 6TM-rH_3 isoforms on the functionality of 7TM-rH_3Rs. To assess the effects of the coexpression of 6TM-rH_3 isoforms on the functionality of 7TM-rH_3Rs, we chose to evaluate H_3R-agonist induced [^{35}S]GTPγS binding to activated Gα proteins. To increase the sensitivity of this assay (Milligan, 2000), we created fusion proteins consisting of the $rH_{3A}R$ fused to one of the PTX-insensitive mutant rat $G\alpha_{i/o}$ proteins: $G\alpha_{i_1}C^{351}I$, $G\alpha_{i_2}C^{352}I$, $G\alpha_{i_3}C^{351}I$, or $G\alpha_oC^{351}I$ (creating $rH_{3A}R$-$G\alpha_{o_1}C^{351}I$, $rH_{3A}R$-$G\alpha_{i_1}C^{351}I$, $rH_{3A}R$-$G\alpha_{i_2}C^{352}I$, and $rH_{3A}R$-$G\alpha_{i_3}C^{351}I$, respectively) by PCR according to *Materials and Methods*.

Characterization of $rH_{3A}R$. Gα fusion proteins—the four different $rH_{3A}R$ fusion proteins $rH_{3A}R$-$G\alpha_{o_1}C^{351}I$, $rH_{3A}R$-$G\alpha_{i_1}C^{351}I$, $rH_{3A}R$-$G\alpha_{i_2}C^{352}I$, and $rH_{3A}R$-$G\alpha_{i_3}C^{351}I$—were subsequently characterized by ^{125}IPP binding assays upon their heterologous expression in COS-7 cells. Based on these studies (data not shown), we decided to continue our experiments using the $rH_{3A}R$-$G\alpha_{o_1}C^{351}I$ fusion protein as this fusion protein exhibited a pK_b value for ^{125}IPP of 8.4 ± 0.2 that corresponds to the obtained pK_b value of ^{125}IPP for the wild-type $rH_{3A}R$ of 8.2 ± 0.1. In addition, the affinities of the wild-type $rH_{3A}R$ and the $rH_{3A}R$-$G\alpha_{o_1}C^{351}I$ fusion protein for the H_3R agonist immepip and the inverse H_3R agonist thioperamide are similar (6.5 ± 0.2 and 7.7 ± 0.1 versus 6.9 ± 0.1 and 7.9 ± 0.1, respectively).

Subsequently, we compared the capability of the $rH_{3A}R$-$G\alpha_{o_1}C^{351}I$ fusion protein to mediate the inhibition of 10 mM forskolin-induced activation of cAMP response element-mediated gene transcription in COS-7 cells. We found the $rH_{3A}R$-$G\alpha_{o_1}C^{351}I$ fusion protein to potently inhibit the forskolin-induced response upon activation with H_3R agonists. In concert with our findings on the wild-type $rH_{3A}R$, treatment of cells cotransfected with cDNAs encoding the $rH_{3A}R$-$G\alpha_{o_1}C^{351}I$ fusion protein and the cAMP response element-reporter gene with varying concentrations of the H_3R agonists immepip, *R*(α)-methylhistamine, and histamine results in the dose-dependent inhibition of 10 mM forskolin-induced firefly luciferase expression by approximately 40% with EC_{50} values of approximately 4, 30, and 76 nM, respectively (Fig. 6A). These data indicate that the $rH_{3A}R$-$G\alpha_{o_1}C^{351}I$ fusion protein is fully functional and shows an $rH_{3A}R$ pharmacology.

Coexpression of $rH_{3A}R$-$G\alpha_{o_1}C^{351}I$ Fusion Proteins and the rH_{3D} Isoform. Consistent with our findings on the coexpression of 7TM-rH_{3A}Rs with the 6TM-rH_3 isoforms (see Fig. 5), coexpression of the $rH_{3A}R$-$G\alpha_{o_1}C^{351}I$ fusion protein together with the rH_{3D} isoform, results in an rH_{3D}-isoform gene-dosage dependent reduction of $rH_{3A}R$-$G\alpha_{o_1}C^{351}I$ fusion protein-derived ^{125}IPP binding sites (Fig. 6B), and the remaining ^{125}IPP binding sites exhibit an $rH_{3A}R$-$G\alpha_{o_1}C^{351}I$-like pharmacological profile (pK_b for ^{125}IPP, 8.5 ± 0.1; pK_i values for immepip and thioperamide, 7.0 ± 0.2 and 7.6 ± 0.1, respectively). The maximal inhibition of $rH_{3A}R$-$G\alpha_{o_1}C^{351}I$-derived ^{125}IPP binding sites, as evaluated by a transfection of cells with an $rH_{3A}R$-$G\alpha_{o_1}$/rH_{3D} isoform cDNA ratio of 1:10 is ~65% (Fig. 6B).

We subsequently assessed the influence of coexpression of the rH_{3D} isoform on the [^{35}S]GTPγS binding induced by

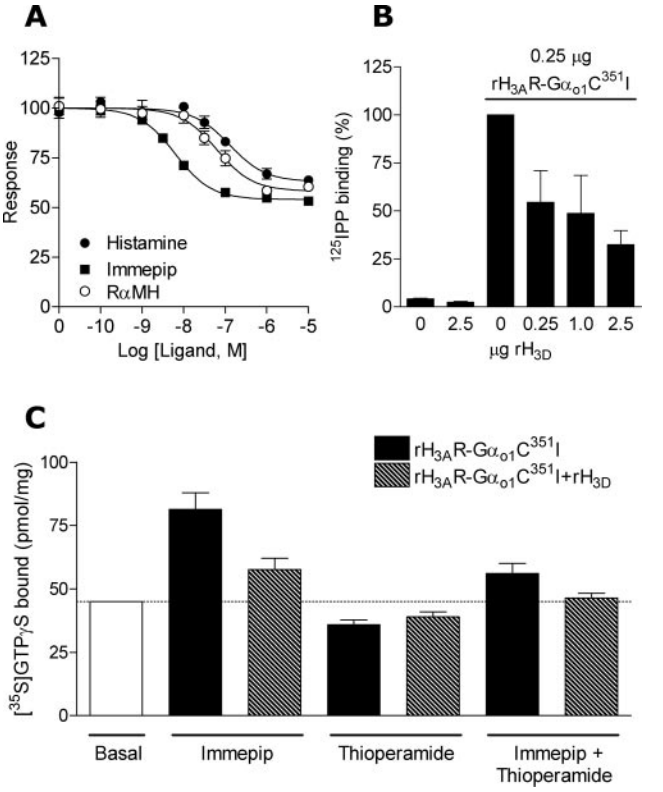

Fig. 6. Effects of cotransfection of the rH_{3D} isoform on the function of the $rH_{3A}R$. A, dose-dependent modulation of 10 mM forskolin induced responses by histamine, immepip, and *R*(α)-methylhistamine using PTX-treated (100 ng/ml) COS-7 cells cotransfected with 5 mg/10^6 cells of both $pcDEF_3rH_{3A}R$-$G\alpha_{o_1}C^{351}I$ and a CREB-responsive firefly-luciferase reporter gene (pTLNC121CRE). B, evaluation of the effects of cotransfection of 0.25 mg/10^6 cells of $pcDEF_3rH_{3A}R$-$G\alpha_{o_1}C^{351}I$ together with varying amounts of $pcDEF_3rH_{3D}$ (0–2.5 mg/10^6 cells) on the relative number of expressed ^{125}IPP binding sites. C, effects of the cotransfection of 0.25 mg/10^6 cells $pcDEF_3rH_{3A}R$ and 2.5 mg/10^6 cells $pcDEF_3rH_{3D}$ on [^{35}S]GTPγS binding to the PTX-insensitive mutant $G\alpha_{o_1}C^{351}I$ protein fused to the C-terminal domain of the $rH_{3A}R$ ($rH_{3A}R$-$G\alpha_{o_1}C^{351}I$ fusion protein). Shown are the effects of cotransfection of $pcDEF_3rH_{3D}$ on the H_3R agonist immepip (1 mM)-induced [^{35}S]GTPγS binding to the $rH_{3A}R$-$G\alpha_{o_1}C^{351}I$ fusion protein in PTX-treated cells (100 ng/ml), and the effects of the inverse H_3R agonist thioperamide (1 mM) on the 1 mM immepip-induced [^{35}S]GTPγS binding. Shown are the averages of three independent experiments.

agonist-mediated activation of coexpressed $rH_{3A}R$-$G\alpha_{o1}C^{351}I$ fusion proteins. The H_3R agonist immepip (1 mM) resulted in a robust stimulation of [^{35}S]GTPγS binding in $rH_{3A}R$-$G\alpha_{o1}C^{351}I$ expressing cells that was inhibited by coincubation with a 1 mM concentration of the inverse H_3R agonist thioperamide (Fig. 6C). Under the assay conditions used, we could not detect significant thioperamide-mediated inhibition of basal $rH_{3A}R$-$G\alpha_{o1}C^{351}I$ mediated [^{35}S]GTPγS binding, indicating that we could not detect constitutive $rH_{3A}R$-$G\alpha_{o1}C^{351}I$ activity. The 1 mM immepip-induced [^{35}S]GTPγS binding was inhibited by 70% by coexpression of the $rH_{3A}R$-$G\alpha_{o1}C^{351}I$ fusion protein with the rH_{3D} isoform (Fig. 6C). The 6TM-rH_3 isoforms themselves did not mediate changes in [^{35}S]GTPγS binding upon incubation with H_3R ligands (data not shown).

Can rH_3Rs Form Homo-Oligomers? In view of the emerging concept of GPCR dimerization that is now well documented in literature (for review, see, for example, Pfleger and Eidne, 2005), we speculated that the 6TM-rH_3 isoforms might interfere with the cell surface expression of 7TM-rH_3 receptors through dimerization.

We have described the generation of anti-rH_{3C} 268–277Cys antibodies (Shenton et al., 2005), which, based on immunoblotting, selectively recognize both the $rH_{3A}R$ and $rH_{3C}R$ isoform, but not the $rH_{3B}R$ isoform expressed in HEK 293 cells. Wild-type $rH_{3A}R$-expressing cells were collected and subjected to cross-linking with varying amounts of the cell permeable cross-linker bis(sulfosuccinimidyl)suberate (BS3) before resolving the samples using SDS-PAGE. Immunoblotting with anti-H_{3C} 268–277Cys antibody yielded three major protein species (M_r 90,000, 135,000, and ~200,000, respectively), corresponding well to putative dimeric, trimeric and tetrameric $rH_{3A}R$ oligomers, respectively (Fig. 7, lanes 1–3). Performing similar experiments using native rat brain tissue, the major species observed is a coincident M_r 90,000 species (Fig. 7, lane 4). It is noteworthy that a recombinant putative monomeric M_r 47,000 species was clearly observed, which was barely detectable in the native forebrain preparation. Higher cross-linker concentrations yielded >200,000 species for both recombinant and native H_3R preparations (Shenton et al., 2005).

We have successfully used the time-resolved FRET (*tr*-FRET) fluorescence (665-nm emission after excitation at 320 nm) for the detection of hH_1R dimerization using epitope-tagged hH_1Rs and fluorescently labeled antibodies recognizing the N-terminally epitope-tagged receptors (Bakker et al., 2004a). We have used this approach to confirm the formation of oligomerization of rH_3Rs.

tr-FRET fluorescence results obtained with the different samples are shown in Fig. 7B. A clear specific *tr*-FRET signal is observed using live cells expressing the HA-$rH_{3A}Rs$. The data are presented as the *tr*-FRET that is observed using HA-$rH_{3A}R$-expressing cells that have been incubated with both anti-HA-Eu^{3+} and anti-HA-allophycocyanin antibodies versus the *tr*-FRET that is observed using a mix of two populations of HA-$rH_{3A}R$-expressing cells that before mixing were independently incubated with either of the two antibodies. The increased *tr*-FRET signal can only be explained by the resonance energy transfer from anti-HA-Eu^{3+} antibodies bound to HA-$rH_{3A}Rs$ to anti-HA-allophycocyanin antibodies bound to HA-$rH_{3A}Rs$, indicative of the formation of $rH_{3A}R$ multimers in living cells.

Modulation of rH_{3AD} and rH_{3DEF} Isoform-Specific mRNAs in Rat Brain after Delivery of a Systemic Convulsant. We have successfully used specific oligonucleotide probes to characterize the 7TM-rH_3R mRNA expression in the rat brain (Drutel et al., 2001). To evaluate the CNS expression of the 6TM-rH_3 isoforms, we have designed domain specific probes. We have used one probe specific for the C terminus present in the 6TM-rH_3 isoforms, and, for comparison, we have also performed studies using a oligonucleotide probe specific for the (full-length) third intracellular loop of the $rH_{3A}R$, which is also present in the rH_{3D} isoform

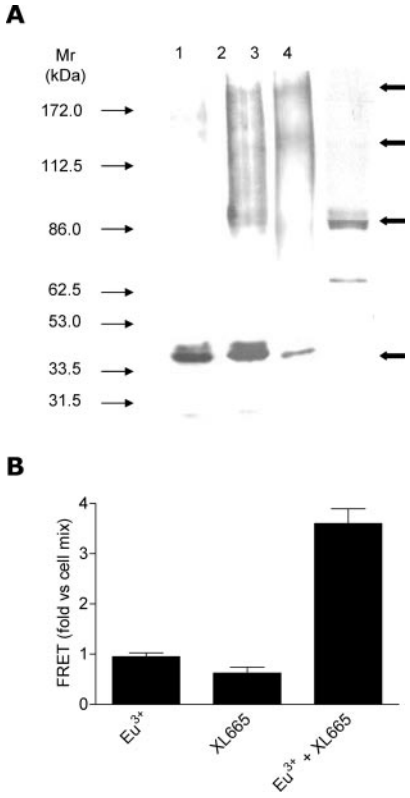

Fig. 7. Detection of oligomerization of heterologous and native $rH_{3A}Rs$. A, biochemical evidence for $rH_{3A}R$ oligomers. Membranes derived from either cells heterologously expressing $rH_{3A}Rs$ or from native rat forebrain membranes were analyzed by immunoblotting (lanes 1–3 and 4, respectively) as described under *Materials and Methods*. In addition, samples of membranes expressing $rH_{3A}Rs$ were subjected to chemical cross-linking with either 0.12 mM or 0.25 mM BS3 (lanes 2 and 3, respectively) before immunoblotting. Lanes 1 to 3 were subsequently probed with rabbit anti-H_{3C} 268–277Cys antibody (0.2 μg/ml), and lane 4 was probed with rabbit anti-H_3 349–358 antibody (1.5 μg/ml). The immunoblot is representative of at least three separate experiments. The molecular mass standards are displayed on the left and are indicated in kilodaltons. B, detection of dimeric $rH_{3A}Rs$ by *tr*-FRET. Upon measuring fluorescence emission at 665 nm, after excitation at 337 nm, *tr*-FRET signals are seen using live cells expressing HA-$rH_{3A}Rs$, because of the resonance energy transfer of specific HA-$rH_{3A}Rs$ bound to anti-HA-Eu^{3+} antibody to the specific HA-$rH_{3A}Rs$ bound to anti-HA-allophycocyanin antibody. *tr*-FRET signals were seen only using membranes of HA-$rH_{3A}R$ expressing cells that were coincubated with both the anti-HA-Eu^{3+} (Eu^{3+}) antibody and the anti-HA-allophycocyanin (XL665) antibody (Eu^{3+} + XL665). Mixing of two populations of cells expressing HA-$rH_{3A}Rs$ independently incubated with either anti-HA-Eu^{3+} or anti-HA-allophycocyanin antibodies resulted in a reduced *tr*-FRET signal. Data are plotted as the *tr*-FRET that is observed using HA-$rH_{3A}R$ expressing cells that have been incubated with both anti-HA-Eu^{3+} and anti-HA-allophycocyanin antibodies versus the *tr*-FRET that is observed using a mix of two populations of HA-$rH_{3A}R$ expressing cells that before mixing were independently incubated with either of the two antibodies.

(but not any of the other rH_3 isoforms identified to date; Fig. 8A).

Significant increases in mRNA expression levels of H_3R isoforms with full-length third intracellular loop (detected using probe H_{3AD}) were observed in layers II-VIb of cortex (48 h after injection), caudate putamen (48 h after injection), piriform cortex (48 h after injection), and CA1 region of the hippocampus (24 h after injection) (Fig. 8B) after PTZ. Figure 8C illustrates mRNA expression levels and differences for H_{3A} and H_{3D} isoforms in representative sections from control and 48 h after injection animals.

In contrast, decreases in mRNA expression pattern of 6TM-rH_3 isoforms (detected using probe H_{3DEF}) were observed in layers II-VIb of cortex (6 h after injection), piriform cortex (6, 24, and 48 after injection), CA1 region of the hippocampus (24 h after injection), and CA3 region of the hippocampus (24 h after injection) (Fig. 8D). Figure 8E shows mRNA expression patterns and differences for 6TM-rH_3 isoforms in representative sections from control animals and animals 24 h after injection.

Discussion

Our search for additional alternative splice variants of the rH_3R resulted in the identification of three mRNAs coding for heretofore uncharacterized rH_3 isoforms. In contrast to the known functional H_3Rs, sequence analysis of these newly identified isoforms reveals that an additional splicing event occurs within a region corresponding to TM6, resulting in isoforms with an alternative C-terminal domain and isoforms that are predicted to possess only 6 TMs. The mRNAs encoding these 6TM-rH_3 isoforms are expressed in the rat brain with a distribution pattern that is similar to the previously identified functional 7TM-rH_3Rs (Drutel et al., 2001). Although there may be differences in the rate of synthesis, the inherent stability, and the rate of degradation of the various H_3 isoforms, resulting in differences in their expression levels, extensive analysis of the 6TM-rH_3 isoforms through heterologous expression studies, however, failed to identify any ligand-binding and functional signaling events modulated by these 6TM-rH_3 isoforms. The 6TM-rH_3 isoforms seem to be localized intracellularly, and succeeding studies revealed the ability of the 6TM-rH_3 isoforms to interfere with the cell surface expression and subsequent signaling of the previously identified 7TM-rH_3 isoforms, thus acting as dominant-negative isoforms.

An increasing number of GPCRs have been shown to exist as oligomeric complexes (for review, see, for example, Pfleger and Eidne, 2005), which are thought to be formed early

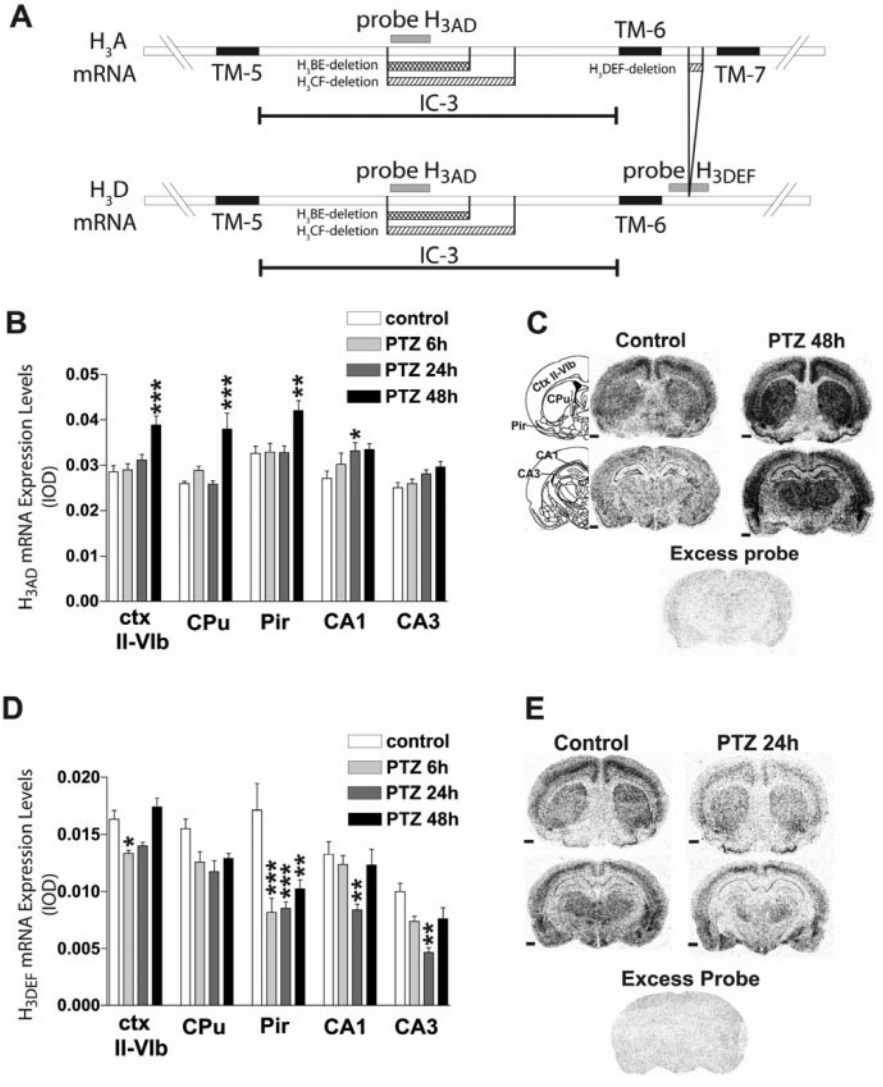

Fig. 8. Detection of rH_3 isoform mRNA in rat brain. A, diagrammatic representation of mRNA sequences recognized by probes H_{3AD} and H_{3DEF}. B, mRNA levels of isoforms detected with probe H_{3AD}. C, images of representative sections from control animals and animals 48 h after PTZ injection. D, expression mRNA levels of isoforms detected with probe H_{3DEF}. E, images of representative sections from control animals and animals 24 h after injection. Data are presented as integrated optic density ± S.E.M.; levels of significance are as follows: *, $p < 0.05$; **, $p < 0.01$; ***, $p < 0.001$. ctx II-VIb, cortex layers II to VIb; CPu, caudate putamen; Pir, piriform cortex; CA1, CA1 region of the hippocampus; CA3, CA3 region of the hippocampus.

during biosynthesis (Terrillon et al., 2003). In this study, we show also that the $rH_{3A}R$ is present as dimers or higher order oligomeric complexes in both transfected cells and rat brain. The oligomerization of GPCRs during biosynthesis and maturation seems crucial for proper exportation of receptors to the plasma membrane (for review, see Bulenger et al., 2005). The coexpression and formation of heterodimeric β_2-ARs (Hague et al., 2004a) aids, for instance, the cell surface trafficking of olfactory GPCRs that are otherwise retained and degraded in the ER (Lu et al., 2003, 2004), as well as of the α_{1D}-AR that normally is trafficked poorly to the cell surface (Uberti et al., 2005). The coexpression of differentially spliced GPCR variants may also aid the cell-surface expression, as shown for instance by the coexpression of the α_{1D}-AR with α_{1B}-ARs (Hague et al., 2004b). In contrast, certain alternatively spliced variants of, for instance, the α_{1A}-AR (Cogé et al., 1999), the calcitonin receptor (Seck et al., 2003), and the dopamine D_3 receptor (Karpa et al., 2000) seem to dimerize with their cognate full-length receptors and impede their cell surface expression because of mislocalization to an intracellular compartment. The coexpression of the 6TM-rH_3 isoforms described herein not only reduced cell surface expression of the 7TM-rH_3Rs but also consequently resulted in a reduced 7TM-rH_3R-mediated signaling. Our data are therefore consistent with the reported findings on the coexpression of N-terminal truncated, dominant-negative mutants and wild-type V_2 receptors, which results in the formation of heterodimers and reduced agonist binding, signal transduction, and cell-surface trafficking of the full-length V_2 receptor (Zhu and Wess, 1998). Similar to our findings on the 6TM-rH_3 isoforms, mutants of the α_2-AR (Zhou et al., 2006), vasopressin V_2 (Zhu and Wess, 1998), dopamine D_2 (Lee et al., 2000), chemokine receptor CCR5 (Benkirane et al., 1997; Blanpain et al., 2000; Chelli and Alizon, 2001), gonadotropin-releasing hormone receptor (Brothers et al., 2004), and the platelet-activating factor (Le Gouill et al., 1999) receptors also impede the cell surface expression of their coexpressed wild-type counterparts, thus exhibiting trans-dominant-negative effects on wild-type receptor expression (Benkirane et al., 1997; Chelli and Alizon, 2001; Brothers et al., 2004), most likely through dimerization. It seems most likely that the 6TM-rH_3 isoforms interfere with the functional expression of the 7TM-rH_3Rs through heterodimerization. Although direct heterodimerization of the 6TM-rH_3 isoforms with the 7TM-rH_3Rs remains to be established, we have shown the $rH_{3A}R$ to be constitutively expressed as a dimeric receptor in the brain as well as upon heterologous expression.

GPCRs have been found to interact with accessory proteins, which can be critical for their biogenesis (for review, see Bermak and Zhou, 2001; Metherell et al., 2005). A conserved $F(X)_6LL$ motif, which is suggested to be important for the proper GPCR folding and subsequent export from the ER (Duvernay et al., 2004), is also present in the C-terminal domain of the 7TM-rH_3Rs but is lacking in the 6TM-rH_3 isoforms. Mutations in regions overlapping the $F(X)_6LL$ motif in the dopamine D_1 receptor resulted in ER retention of the mutant receptor and loss of cell surface expression, and subsequent studies revealed that this region is important for a interactions with a specific ER-membrane-associated protein that regulates transport of GPCRs (Bermak et al., 2001). It is noteworthy that, instead of the $F(X)_6LL$ motif, the 6TM-rH_3 isoforms possess an RXR ER retention signal. Taken together, these data suggest that the 6TM-rH_3 isoforms lack protein-protein interactions with specific accessory proteins in the ER that are required for cell-surface expression. Although the localization of the 6TM-rH_3 isoforms within the ER seems likely, this needs to be verified by future experiments. Nonetheless, the findings on GPR30 as an intracellular GPCR (Revankar et al., 2005) points out that the 6TM-rH_3 isoforms may well have yet undiscovered intracellular functions in addition to their capability to retain the 7TM-rH_3Rs intracellularly.

On the one hand, the 6TM-rH_3 splice variants may act as "antichaperones" inhibiting specific chaperones' activities or preventing their access to the 7TM-rH_3Rs. On the other hand, the association of the 6TM-rH_3 isoforms with the 7TM-rH_3R isoforms in the ER may actively unfold or result in the misfolding of the protein complex. Because we find that the rH_{3D} isoform does not interfere with the cell surface expression of unrelated GPCRs, it seems unlikely the 6TM-rH_3 isoforms act through blocking either the ER or Golgi, or to promote ER-associated protein degradation. The precise mechanism underlying the action of the newly identified isoforms, however, remains unknown. Our data suggest that the regulation of the alternative rH_3R mRNA splicing is a new and effective means for the regulation of H_3R signaling. Functional (including constitutive) H_3R activity may be regulated through the regulation of the splicing events underlying the occurrence of the various H_3R isoforms. It is noteworthy that several cell signaling pathways, including the MAPK pathway, regulate mRNA splicing (reviewed in Shin and Manley, 2004). It is intriguing that the H_3R activates the MAPK pathway (Drutel et al., 2001; Giovannini et al., 2003), arguing for the possibility of activation of splicing factors and hence, an autoregulation of the H_3R activity.

Our studies also show that the expression pattern of the 7TM-rH_3Rs and the 6TM-rH_3 isoforms overlaps substantially in rat brain. Moreover, PTZ-induced seizures result in suppression of 6TM-rH_3 (probe H_{3DEF}) isoform mRNAs in particular brain regions, whereas mRNA levels of the isoforms with the full third intracellular loop (probe H_{3AD}) are increased. A characteristic transient and short-living increase in the mRNA for the full-length third intracellular loop (probe H_{3AD}), hippocampal CA_{3c} area, followed by piriform cortex, amygdala, and hippocampal CA_1 area is observed after systemic injection of kainic acid, a model of temporal lobe epilepsy (Lintunen et al., 2005), indicating a spatiotemporal correlation to progressing neuronal damage in this model of temporal epilepsy. Previous studies on PTZ have indicated damaged neurons in the rostral limbic cortex (both the orbital, agranular insular, and prelimbic), the lateral hypothalamus (in the vicinity of the rostral medial forebrain bundle), the bed nucleus of the stria terminalis, the claustrum, the hippocampal formation (CA3 and entorhinal cortex), and lateral thalamic nuclei 50 min after injection (Ben-Ari et al., 1981). The increases in H_3R mRNA with full third intracellular loop as observed in this study after PTZ were observed significantly later than the reported damage begins (Ben-Ari et al., 1981), in agreement with the concept that the mechanisms of neuronal damage after kainic acid and PTZ are different. Although the piriform cortex has not been reported to suffer significant damage after PTZ (Ben-Ari et al., 1981), it seems not to be only a primary sensory area but because of its neuronal organization and associative

fiber system may also be involved in the pathological mechanisms leading to seizures (Löscher and Ebert, 1996). Of the areas studied here, the piriform cortex showed a sustained decline in 6TM-rH_3 mRNA expression. We observed a significant transient increase in H_3R radioligand binding in piriform cortex at 6 h after PTZ concomitantly with the decline of H_{3DEF} isoform mRNAs (data not shown). However, a similar strong correlation was not found in all areas where smaller changes were seen, suggesting that other factors in addition to mRNA ratios may affect receptor binding. The high susceptibility for induction of seizures by chemical or electrical stimulation and various studies addressing its role in seizure generation suggest that the piriform cortex can also function as an amplifier region to increase and propagate seizure activity induced in other limbic regions (Löscher and Ebert, 1996). Increased H_3R activity (e.g., expression and translation) in this region could result in decreased glutamate release (Brown and Haas, 1999; Molina-Hernandez et al., 2001), because glutamatergic neurons exist in the piriform cortex (Riba-Bosch and Perez-Clausell, 2004), for control of overall neuronal activity in the region.

The abundance of mRNA coding for the 6TM-rH_3 isoforms suggest that its production may have important biological implications. For example, in addition to its ability to interfere with cell surface expression of functional rH_3Rs, which may arise from modification of the stability of the mRNA encoding functional 7TM-rH_3Rs, the 6TM-rH_3 isoform mRNAs might encode proteins with yet unidentified functions. Further analysis of the alternatively spliced products of the H_3R gene is required to elucidate their biological significance.

In conclusion, we have identified three additional splice variants of the rH_3R. The mRNAs of these isoforms are abundantly expressed in the brain and the expression pattern largely overlaps with that of the known r$H_{3A\text{-}C}$R isoforms. Analysis of the sequence of these rH_{3D}, rH_{3E}, and rH_{3F} isoforms reveals these isoforms to consist of 6TM domains. The 6TM-rH_3 isoforms are retained intracellularly upon heterologous expression, and in subsequent pharmacological analysis studies we could detect no ligand binding or functional activity for these 6TM-rH_3 isoforms. The 6TM-rH_3 isoforms, however, selectively impede cell surface expression of the functional 7TM-rH_3Rs. Moreover, the mRNA levels of the rH_3 isoforms in rat brain are modulated by treatment with the convulsant PTZ. Although the functional significance and possible roles of these 6TM-rH_3 isoforms in (patho)physiology remain to be established, these findings provide novel insight in the regulation of the histaminergic system in the brain.

Acknowledgments

This article is dedicated to Dr. Art A. Hancock, who passed away on November 11, 2005. Dr. Hancock was a great scientist with a warm and generous personality. Under his inspired leadership, Abbott Laboratories made many seminal contributions to the field of H_3 receptors.

We thank Sarina M. Meusburger, Franca di Summa, Kim Retra, and José Antonio Arias-Montaño for expert assistance.

References

Bakker RA (2004) Histamine H_3-receptor isoforms. *Inflamm Res* **53:**509–516.

Bakker RA, Dees G, Carrillo JJ, Booth RG, López-Gimenez JF, Milligan G, Strange PG, and Leurs R (2004a) Domain swapping in the human histamine H_1 receptor. *J Pharmacol Exp Ther* **311:**131–138.

Bakker RA, Weiner DM, ter Laak T, Beuming T, Zuiderveld OP, Edelbroek M, Hacksell U, Timmerman H, Brann MR, and Leurs R (2004b) 8R-Lisuride is a potent stereospecific histamine H_1-receptor partial agonist. *Mol Pharmacol* **65:** 538–549.

Ben-Ari Y, Tremblay E, Riche D, Ghilini G, and Naquet R (1981) Electrographic, clinical and pathological alterations following systemic administration of kainic acid, bicuculline or pentetrazole: metabolic mapping using the deoxyglucose method with special reference to the pathology of epilepsy. *Neuroscience* **6:**1361–1391.

Benkirane M, Jin DY, Chun RF, Koup RA, and Jeang KT (1997) Mechanism of transdominant inhibition of CCR5-mediated HIV-1 infection by ccr5D32. *J Biol Chem* **272:**30603–30606.

Bermak JC, Li M, Bullock C, and Zhou QY (2001) Regulation of transport of the dopamine D1 receptor by a new membrane-associated ER protein. *Nat Cell Biol* **3:**492–498.

Bermak JC and Zhou QY (2001) Accessory proteins in the biogenesis of G protein-coupled receptors. *Mol Intervent* **1:**282–287.

Blanpain C, Lee B, Tackoen M, Puffer B, Boom A, Libert F, Sharron M, Wittamer V, Vassart G, Doms RW, et al. (2000) Multiple nonfunctional alleles of CCR5 are frequent in various human populations. *Blood* **96:**1638–1645.

Brothers SP, Cornea A, Janovick JA, and Conn PM (2004) Human loss-of-function gonadotropin-releasing hormone receptor mutants retain wild-type receptors in the endoplasmic reticulum: molecular basis of the dominant-negative effect. *Mol Endocrinol* **18:**1787–1797.

Brown RE and Haas HL (1999) On the mechanism of histaminergic inhibition of glutamate release in the rat dentate gyrus. *J Physiol* **515 (Pt 3):**777–786.

Bulenger S, Marullo S, and Bouvier M (2005) Emerging role of homo- and heterodimerization in G-protein-coupled receptor biosynthesis and maturation. *Trends in Pharmacological Sciences* **26:**131–137.

Chazot PL, Hann V, Wilson C, Lees G, and Thompson CL (2001) Immunological identification of the mammalian H_3 histamine receptor in the mouse brain. *Neuroreport* **12:**259–262.

Chelli M and Alizon M (2001) Determinants of the *trans*-dominant negative effect of truncated forms of the CCR5 chemokine receptor. *J Biol Chem* **276:**46975–46982.

Cogé F, Guénin SP, Audinot V, Renouard-Try A, Beauverger P, Macia C, Ouvry C, Nagel N, Rique H, Boutin JA, et al. (2001) Genomic organization and characterization of splice variants of the human histamine H_3 receptor. *Biochem J* **355:** 279–288.

Cogé F, Guenin SP, Renouard-Try A, Rique H, Ouvry C, Fabry N, Beauverger P, Nicolas JP, Galizzi JP, Boutin JA, et al. (1999) Truncated isoforms inhibit [^{3}H]prazosin binding and cellular trafficking of native human a_{1A}-adrenoceptors. *Biochem J* **343:**231–239.

Drutel G, Peitsaro N, Karlstedt K, Wieland K, Smit MJ, Timmerman H, Panula P, and Leurs R (2001) Identification of rat H_3 receptor isoforms with different brain expression and signaling properties. *Mol Pharmacol* **59:**1–8.

Duvernay MT, Zhou F, and Wu G (2004) A conserved motif for the transport of G protein-coupled receptors from the endoplasmic reticulum to the cell surface. *J Biol Chem* **279:**30741–30750.

Giovannini MG, Efoudebe M, Passani MB, Baldi E, Bucherelli C, Giachi F, Corradetti R, and Blandina P (2003) Improvement in fear memory by histamine-elicited ERK2 activation in hippocampal CA3 cells. *J Neurosci* **23:**9016–9023.

Hague C, Uberti MA, Chen Z, Bush CF, Jones SV, Ressler KJ, Hall RA, and Minneman KP (2004a) Olfactory receptor surface expression is driven by association with the β_2-adrenergic receptor. *Proc Natl Acad Sci USA* **101:**13672–13676.

Hague C, Uberti MA, Chen Z, Hall RA, and Minneman KP (2004b) Cell surface expression of α_{1D}-adrenergic receptors is controlled by heterodimerization with α_{1B}-adrenergic receptors. *J Biol Chem* **279:**15541–15549.

Hawrylyshyn KA, Michelotti GA, Coge F, Guenin SP, and Schwinn DA (2004) Update on human alpha1-adrenoceptor subtype signaling and genomic organization. *Trends Pharmacol Sci* **25:**449–455.

Karpa KD, Lin R, Kabbani N, and Levenson R (2000) The dopamine D3 receptor interacts with itself and the truncated D3 splice variant d3nf: D3–D3nf interaction causes mislocalization of D3 receptors. *Mol Pharmacol* **58:**677–683.

Kilpatrick GJ, Dautzenberg FM, Martin GR, and Eglen RM (1999) 7TM receptors: the splicing on the cake. *Trends Pharmacol Sci* **20:**294–301.

Lee SP, O'Dowd BF, Ng GY, Varghese G, Akil H, Mansour A, Nguyen T, and George SR (2000) Inhibition of cell surface expression by mutant receptors demonstrates that D2 dopamine receptors exist as oligomers in the cell. *Mol Pharmacol* **58:**120–128.

Le Gouill C, Parent JL, Caron CA, Gaudreau R, Volkov L, Rola-Pleszczynski M, and Stankova J (1999) Selective modulation of wild type receptor functions by mutants of G-protein-coupled receptors. *J Biol Chem* **274:**12548–12554.

Leurs R, Bakker RA, Timmerman H, and de Esch IJ (2005) The histamine H_3 receptor: from gene cloning to H_3 receptor drugs. *Nat Rev Drug Discov* **4:**107–120.

Lintunen M, Sallmen T, Karlstedt K, and Panula P (2005) Transient changes in the limbic histaminergic system after systemic kainic acid-induced seizures. *Neurobiol Dis* **20:**155–169.

Löscher W and Ebert U (1996) The role of the piriform cortex in kindling. *Prog Neurobiol* **50 (5–6):**427–481.

Lu M, Echeverri F, and Moyer BD (2003) Endoplasmic reticulum retention, degradation and aggregation of olfactory G-protein coupled receptors. *Traffic* **4:**416–433.

Lu M, Staszewski L, Echeverri F, Xu H, and Moyer BD (2004) Endoplasmic reticulum degradation impedes olfactory G-protein coupled receptor functional expression. *BMC Cell Biol* **5:**34.

Metherell LA, Chapple JP, Cooray S, David A, Becker C, Ruschendorf F, Naville D, Begeot M, Khoo B, Nurnberg P, et al. (2005) Mutations in MRAP, encoding a new

interacting partner of the ACTH receptor, cause familial glucocorticoid deficiency type 2. *Nat Genet* **37:**166–170.
Milligan G (2000) Insights into ligand pharmacology using receptor-G-protein fusion proteins. *Trends Pharmacol Sci* **21:**24–28.
Molina-Hernandez A, Nunez A, Sierra JJ, and Arias-Montano JA (2001) Histamine H_3 receptor activation inhibits glutamate release from rat striatal synaptosomes. *Neuropharmacology* **41:**928–934.
Morisset S, Sasse A, Gbahou F, Héron A, Ligneau X, Tardivel-Lacombe J, Schwartz JC, and Arrang JM (2001) The rat H_3 receptor: gene organization and multiple isoforms. *Biochem Biophys Res Commun* **280:**75–80.
Pfleger KD and Eidne KA (2005) Monitoring the formation of dynamic G-protein-coupled receptor-protein complexes in living cells. *Biochem J* **385:**625–637.
Revankar CM, Cimino DF, Sklar LA, Arterburn JB, and Prossnitz ER (2005) A transmembrane intracellular estrogen receptor mediates rapid cell signaling. *Science (Wash DC)* **307:**1625–1630.
Riba-Bosch A and Perez-Clausell J (2004) Response to kainic acid injections: changes in staining for zinc, FOS, cell death and glial response in the rat forebrain. *Neuroscience* **125:**803–818.
Schmauss C, Haroutunian V, Davis KL, and Davidson M (1993) Selective loss of dopamine D_3-type receptor mRNA expression in parietal and motor cortices of patients with chronic schizophrenia. *Proc Natl Acad Sci USA* **90:**8942–8946.
Seck T, Baron R, and Horne WC (2003) The alternatively spliced De13 transcript of the rabbit calcitonin receptor dimerizes with the C1a isoform and inhibits its surface expression. *J Biol Chem* **278:**23085–23093.
Shenton FC, Hann V, and Chazot PL (2005) Evidence for native and cloned H_3 histamine receptor higher oligomers. *Inflammation Res* **54:**S48–S49.
Shin C and Manley JL (2004) Cell signalling and the control of pre-mRNA splicing. *Nat Rev Mol Cell Biol* **5:**727–738.
Smit MJ, Verzijl D, Casarosa P, Navis M, Timmerman H, and Leurs R (2002) Kaposi's sarcoma-associated herpesvirus-encoded G protein-coupled receptor ORF74 constitutively activates p44/p42 MAPK and Akt via G_i and phospholipase C-dependent signaling pathways. *J Virol* **76:**1744–1752.
Terrillon S, Durroux T, Mouillac B, Breit A, Ayoub MA, Taulan M, Jockers R, Barberis C, and Bouvier M (2003) Oxytocin and vasopressin V1a and V2 receptors form constitutive homo- and heterodimers during biosynthesis. *Mol Endocrinol* **17:**677–691.
Uberti MA, Hague C, Oller H, Minneman KP, and Hall RA (2005) Heterodimerization with b_2-adrenergic receptors promotes surface expression and functional activity of a_{1D}-adrenergic receptors. *J Pharmacol Exp Ther* **313:**16–23.
White JH, Wise A, Main MJ, Green A, Fraser NJ, Disney GH, Barnes AA, Emson P, Foord SM, and Marshall FH (1998) Heterodimerization is required for the formation of a functional $GABA_B$ receptor. *Nature (Lond)* **396:**679–682.
Zhou F, Filipeanu CM, Duvernay MT, and Wu G (2006) Cell-surface targeting of α_2-adrenergic receptors—inhibition by a transport deficient mutant through dimerization. *Cell Signal* **18:**318–327.
Zhu X and Wess J (1998) Truncated V_2 vasopressin receptors as negative regulators of wild-type V_2 receptor function. *Biochemistry* **37:**15773–15784.

Address correspondence to: Prof. Dr. R. Leurs, The Leiden/Amsterdam Center for Drug Research, Department of Medicinal Chemistry, Vrije Universiteit Amsterdam, De Boelelaan 1083, 1081HV Amsterdam, The Netherlands. E-mail: r.leurs@few.vu.nl